

Effect of the Concentration of Carbonate Groups in a Carbonate Hydroxyapatite Ceramic on Its *In Vivo* Behavior

V. S. Komlev^a, I. V. Fadeeva^a, A. N. Gurin^b, E. S. Kovaleva^c, V. V. Smirnov^a,
N. A. Gurin^b, and S. M. Barinov^a

^a Baikov Institute of Metallurgy and Materials Science, Russian Academy of Sciences, Moscow, Russia

^b Central Scientific Research Institute of Stomatology and Maxillofacial Surgery, Rosmedtekhologii, Moscow, Russia

^c Moscow State University, Moscow, Russia

e-mail: komlev@mail.ru

Received May 13, 2008

Abstract—Carbonate-substituted hydroxyapatites containing up to 9 wt % of carbonate groups were synthesized and fabricated in the form of porous granules with a view to developing materials for use in bone tissue repairs. The use of sintering additives forming a liquid phase allowed the granule sintering temperature to be reduced by 400–450°C. It was found that the carbonate groups enter into the structure of the ceramic by a mixed AB-type substitution; the microstructure of the granules depends substantially on the concentration of the carbonate groups; introduction of 6 wt % of carbonate groups into apatite ensures high biological properties of the granules in experiments *in vivo*.

DOI: 10.1134/S0020168509030194

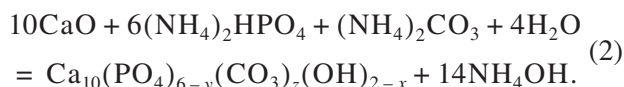
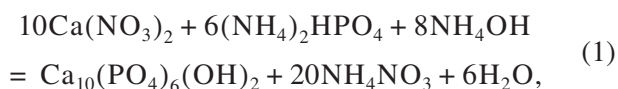
INTRODUCTION

Calcium phosphate materials are used in medicine for the regeneration of damaged bone tissues by way of gradual replacement of the material by the newly growing bone tissue. Hydroxyapatite (HA) used for this purpose today features a slow biological resorption rate—a considerable shortcoming of the material. The resorption process can be enhanced through replacement of the phosphate and hydroxide anions in the apatite structure with carbonate groups [1]. Carbonate-substituted hydroxyapatites (CHA) are similar in composition and structure to the mineral components of natural bone tissue, which contain up to 8 wt % of carbonate groups. The *in vivo* behavior of the ceramic depends on the amount, size, and interconnectivity of pores that facilitate biological currents and improve the adsorption of proteins and adhesion of osteogenetic cells [2–6].

This paper presents the results of a comparative investigation for the structure and biological behavior of CHA granules.

EXPERIMENTAL

HA and CHA powders with a calculated CO_3^{2-} concentration of 0.6, 6, and 9 wt % were synthesized by the reactions



The synthesized powders were made into spherical granules by the suspension method [4, 7]. To reduce the granule sintering temperature and prevent the CHA from decomposition, up to 8 wt % of alkaline or alkaline-earth carbonates were introduced into the CHA powders prior to granulation. Following sintering in a resistance furnace, the granules were screened according to size.

The phase analysis of samples was carried out by CuK_α radiation with a Shimadzu XRD-600 diffractometer. The IR absorption spectra of the samples were recorded in the range 400–4000 cm^{-1} with a Vertex-70 instrument. The solubility of the granules was investigated in a 0.9% isotonic saline solution with an Ekspert-001 analyzer for up to 21 days. Their surface was studied with a TemScan scanning electron microscope.

The effect of ceramic granules on the *in vivo* processes in bone tissue was evaluated on the condyles of rats of the strain Vistar 180–200 g in weight. A perforation 1.5 mm in diameter and 3 mm long was modeled and filled with the material under study. The experiment lasted for 2, 4, and 8 weeks. Upon completion of the experiment, samples were taken from the animals, fixed in formalin, decalcified, dehydrated, and embedded in paraffin wax to prepare serial sections 5–7 μm in thickness. The sections obtained were stained with hematoxylin and eosin and studied under a DM-111

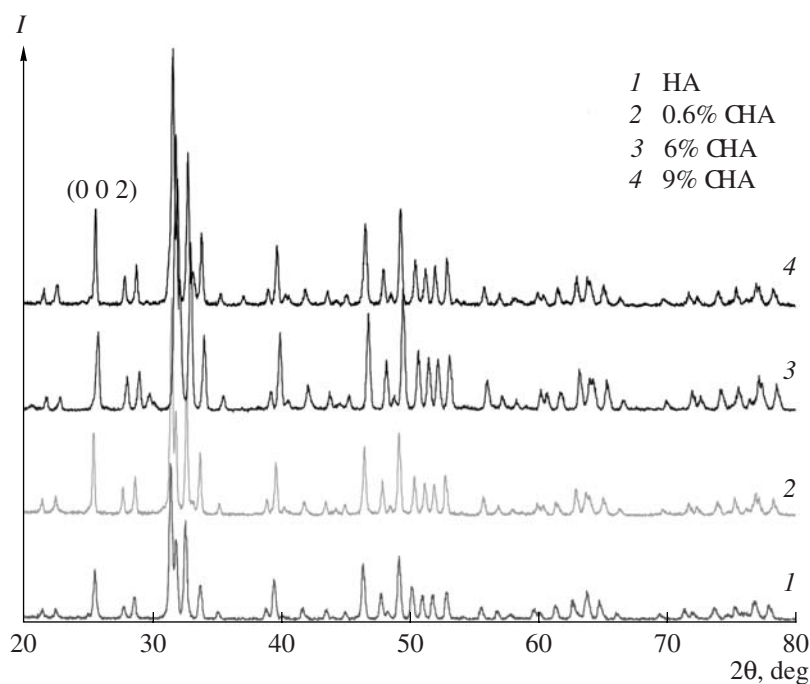


Fig. 1. Diffractograms of calcium phosphate granules.

microscope (Motic Digital Microscopy) equipped with a Macintosh digital camera. Presented in this work are the results of two-week studies.

RESULTS AND DISCUSSION

The x-ray phase analysis of the CHA powders (Fig. 1) showed a spectral similarity to HA, with the respective reflections slightly shifted as a result of the carbonate ions entering into the apatite structure, causing lattice deformations owing to the replacement of PO_4^{3-} and OH^- with CO_3^{2-} .

The characteristics of the granules are presented in Table 1. The use of low-melting additives forming a liquid phase on sintering made it possible to lower the granule sintering temperature to 700–750°C, which is

approximately 400°C below the sintering temperature of CHA granules without such additives, and thus prevent CHA from thermal decomposition.

The IR spectroscopy of the HA and CHA granules revealed the presence of absorption bands characteristic of these compounds (Fig. 2). The positions of the absorption bands in the spectra are indicated in Table 2. With the CO_3^{2-} content of CHA amounting to 0.6 wt %, the intensity of the OH^- vibrations at 636 cm^{-1} is substantially reduced; the same is true of the ν_4 vibrations in PO_4^{3-} at 603 and 568 cm^{-1} ; also lowered is the intensity of the absorption band of OH^- at 3570 cm^{-1} . Weak ν_3 CO_3^{2-} absorption bands appear at 1460 and 1417 cm^{-1} . For CHA containing 6 wt % CO_3^{2-} , no OH^- absorption band (636 cm^{-1}) is observed; the intensity of the ν_2

Table 1. Characteristics of synthesized granules

Granules	Size of granules, mm	Granule surface	External pores, μm	Internal pores, μm
HA	0.5–1.0	Dendritic	<10	30–400
0.6%-substituted CHA	0.5–1.0	Acicular-lamellar	<10	up to 500
6%-substituted CHA	0.6–1.0	Hexagonal crystals	<10	≈ 300
9%-substituted CHA	0.3–0.8	Hexagonal crystals	<10	30–400

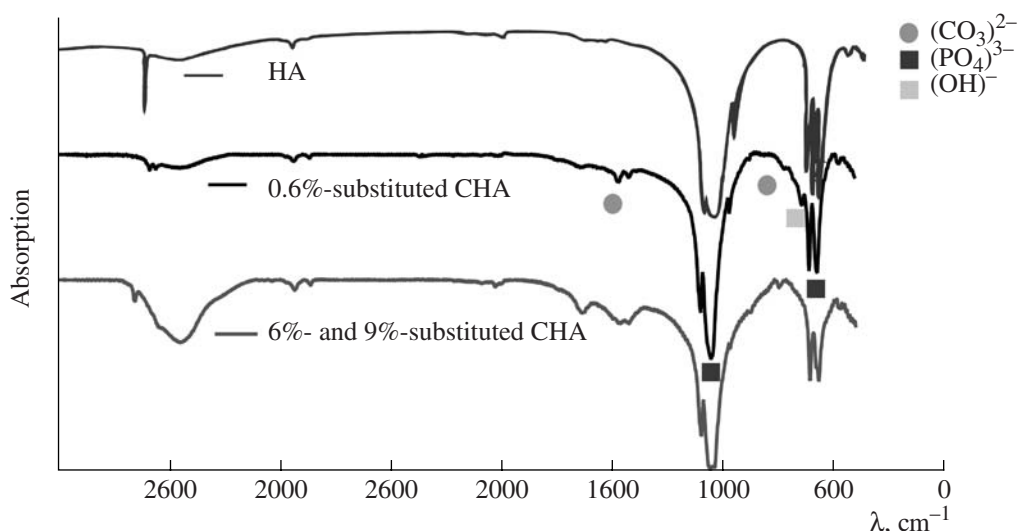


Fig. 2. IR absorption spectra of HA (absence of absorption bands of CO_3^{2-} groups); 0.6%-substituted CHA (appearance of weak absorption bands at 870, 1417, and 1460 cm^{-1}); and 6%- and 9%-substituted CHA (absence of the absorption band at 632 cm^{-1} , increase in the absorption intensity at 870, 1417, and 1460 cm^{-1}).

CO_3^{2-} band at 870 cm^{-1} grows somewhat higher, and so does the intensity of the $\nu_3 \text{CO}_3^{2-}$ bands at 1460 and 1420 cm^{-1} (Fig. 2c). CHA with 9% substitution (Fig. 2d) exhibits a decrease in the intensity of the $\nu_4 \text{PO}_4^{3-}$ bands at 1090 and 1045 cm^{-1} and of the $\nu_4 \text{PO}_4^{3-}$ bands at 455 and 443 cm^{-1} , an increase in the intensity of the $\nu_2 \text{CO}_3^{2-}$ band at 870 cm^{-1} and of the $\nu_3 \text{CO}_3^{2-}$ bands at 1460 and 1417 cm^{-1} , and the absence of the OH^- absorption band at 636 cm^{-1} . An analysis of the spectra of CHA granules differing in the degree of substitution has shown that, as the concentration of the carbonate groups in the structure of the material grows higher, the OH^- and PO_4^{3-} groups are gradually replaced by CO_3^{2-} , and absorption frequencies typical of the AB-type carbonate-substituted hydroxyapatite come into existence.

Studies of the solubility of the material obtained in a 0.9% NaCl solution showed CHA containing 9 wt % CO_3^{2-} to have the highest solubility (Fig. 3). After the lapse of 14 days, the Ca^{2+} concentration in all samples leveled out; i.e., the active dissolution period came to an end. The carbonate groups cause lattice deformations, which leads to an increase in solubility [7, 8]. The sintered HA granules remain practically undissolved.

The scanning electron microscopy of the sections of sintered HA granules revealed the presence of large microcavities some 300 μm across inside all of the samples (Fig. 4a, inset). The microstructure of the granules varies depending on the concentration of the carbonate groups. The CHA granules with 0.6 wt % CO_3^{2-} are

represented by hard concretions with open micropores around 2–4 μm in size and nonuniform surface. An acicular-lamellar structure is formed in some areas (Fig. 4b), while in others crystals of irregular shape form the surface. Examination of the internal and exter-

Table 2. Absorption frequencies in the IR spectra of the material under study

Material studied	Absorption frequency, cm^{-1}			
	PO_4^{3-}		CO_3^{2-}	OH^-
HA	ν_1 963	ν_4 602	—	632
		572		
0.6%-substituted CHA	ν_1 962	ν_3 1090	ν_2 873	3434
		1045		3671
6%-substituted CHA	ν_1 962	ν_4 603	ν_2 873	3435
		568		
9%-substituted CHA	ν_1 963	ν_3 1092	ν_3 1416	3435
		1044		3571
6%-substituted CHA	ν_1 962	ν_4 603	ν_2 873	3435
		568		
9%-substituted CHA	ν_1 963	ν_3 1092	ν_3 1416	3435
		1045		3570
0.6%-substituted CHA	ν_1 962	ν_4 603	ν_2 873	3435
		568		
9%-substituted CHA	ν_1 963	ν_3 1092	ν_3 1416	3435
		1045		3571

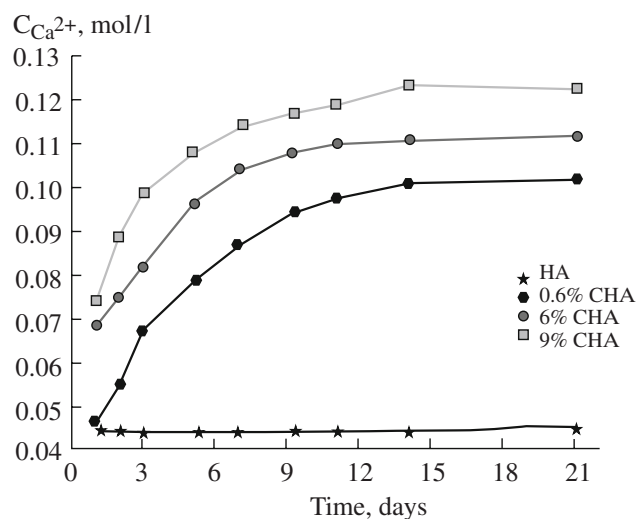


Fig. 3. Concentration of Ca^{2+} ions in isotonic saline solution upon dissolution of calcium phosphate granules.

nal areas of the granules showed them to be constituted of small conglomerates that unite to form the granule. Macrocavities some $300\text{ }\mu\text{m}$ across and fine micropores around $3\text{ }\mu\text{m}$ in size can be seen in cross sections. The central internal areas contain distinctly faceted crystals of hexagonal shape.

The microstructure of the CHA granules containing 6 and 9 wt % CO_3^{2-} features open micropores up to $10\text{ }\mu\text{m}$ in size. The surface is represented by uniform hexagonal crystals of regular shape (Figs. 4c, 4d). All the granules are characterized by macrocavities differing in size. The internal structure of these macrocavities is also represented by crystals of hexagonal shape (some $2\text{ }\mu\text{m}$ on a face).

The general trend is the change in the microstructure of the granules from a dense dendritic to a lamellar-acicular pattern and then to the formation of hexagonal crystals as the concentration of the carbonate groups in CHA grows higher. Similar results were obtained in [9,

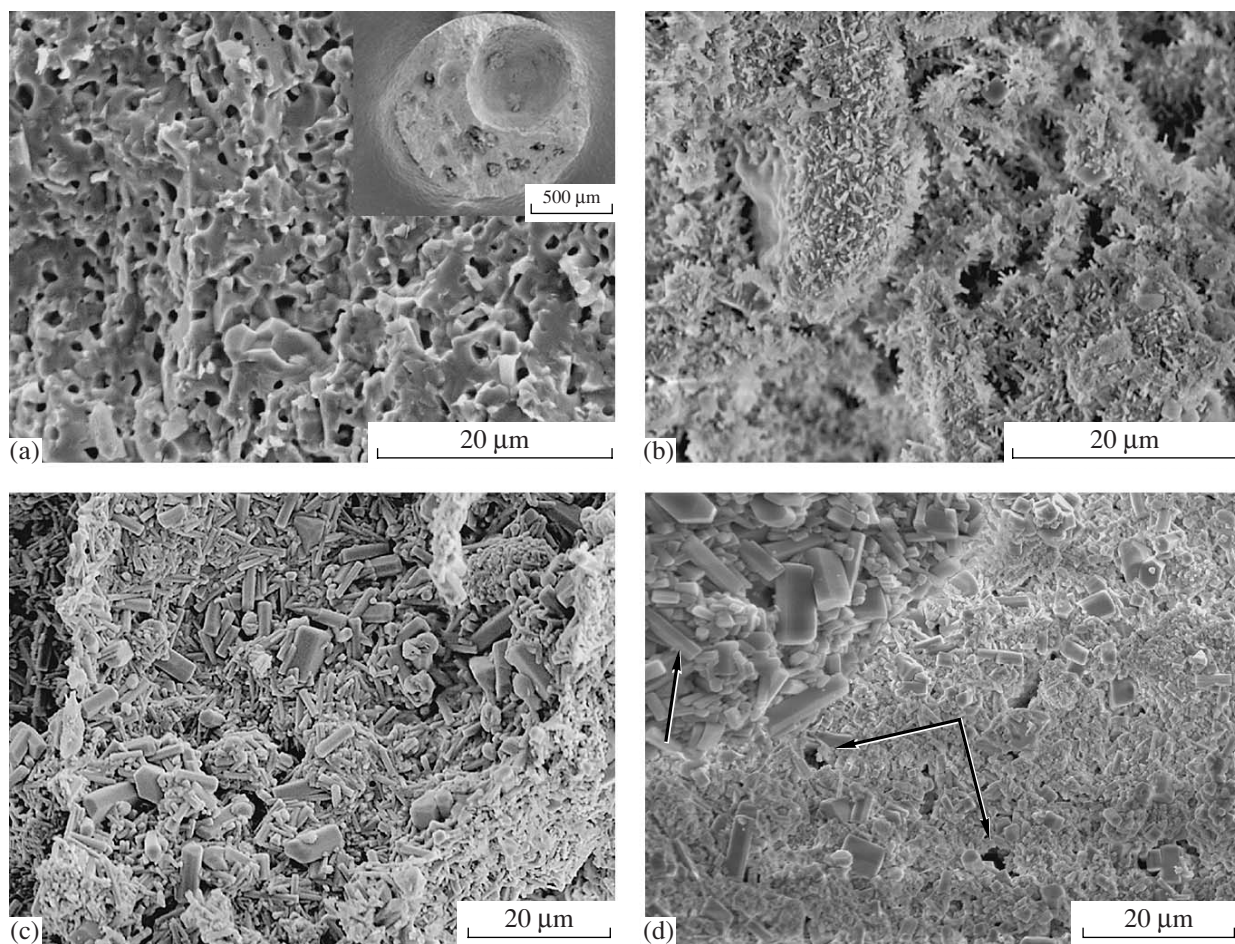


Fig. 4. Results of scanning electron microscopy of calcium phosphate granules: (a) HA (dense fine-pore dendritic structure); inset: cross section with macrocavities characteristic of all the granules studied; (b) 0.6%-substituted CHA (acicular-lamellar surface structure); (c, d) 6%- and 9%-substituted CHA (structure of hexagonal crystals is indicated by single arrows; double arrows indicate micropores).

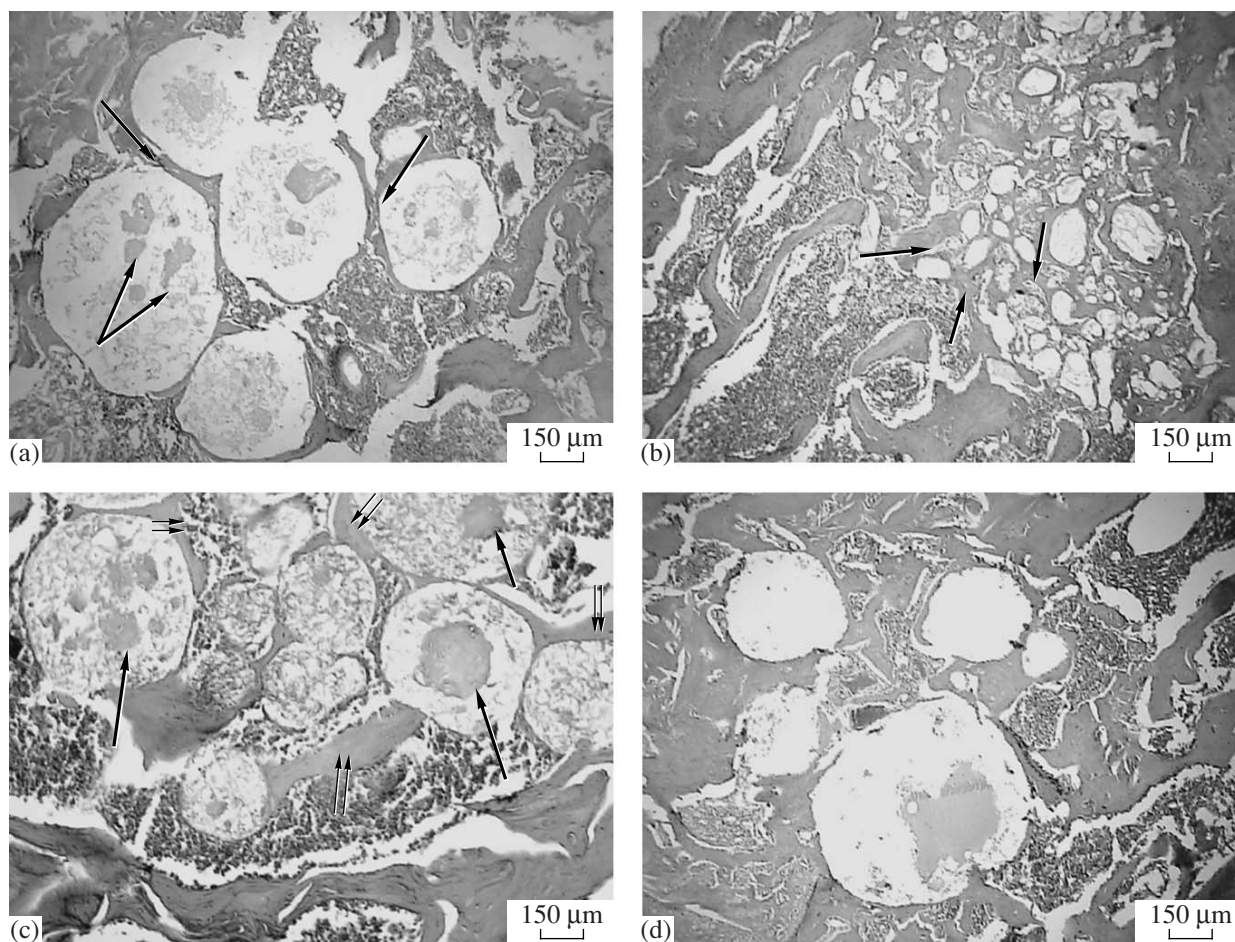


Fig. 5. Histological sections (two-week-long experiment, center of the perforation): (a) HA (single arrows indicate beginning of formation of bone trabecules over the surface of granules; double arrows indicate tissue exudation inside the granules); (b) 0.6%-substituted CHA (resorption of granules into fine fragments and their assimilation by bone tissue, indicated by arrows); (c) 6%-substituted CHA (formation of osteoid tissue with cellular elements inside granules, indicated by single arrows; newly forming bone, indicated by double arrows); (d) 9%-substituted CHA.

10] in studying CHA differing in the degree of substitution.

Investigation into the histological sections of HA granules has demonstrated that the formation of a bone matrix on their surface proceeds at a slow pace. The absence of cellular infiltration into implants is due to the small size of the pores (less than 10 μm). However, there takes place diffusion of the tissue fluid that accumulates in the internal macrocavities. The arrows in Fig. 5a indicate thin interlayers of newly formed bone tissue both between granules and on their surface.

When studying the histological sections of the CHA granules containing 0.6 wt % CO_3^{2-} , we found that they suffered resorption (Fig. 5b). This might be associated with a decrease in the crystallinity of apatite and, hence, an increase in its solubility [7, 8]. Almost no infiltration of the cellular elements into small granules was observed, the diffusion of the tissue fluid being only weakly expressed, possibly because of the closure of pores on the surface.

In the case of implantation of CHA granules containing 6 wt % CO_3^{2-} , the tissue fluid and cellular elements are observed to infiltrate into the material to form osteoid tissue (Fig. 5c). Bone tissue in the form of trabecules originates between the granules.

The histological pattern in the study of CHA with 9 wt % CO_3^{2-} is similar to that in the case of granules containing 6 wt % CO_3^{2-} (Fig. 5d). Most of the granules are impregnated with the tissue fluid. The cellular elements are almost undefinable. New bone tissue actively forms between the granules. The original (native) bone tissue assimilates the adjoining deposits. However, preliminary histological results have shown that the formation of the bone matrix is most expressed in samples containing 6 wt % CO_3^{2-} , wherein the ingrowth of the cellular elements into the granules proceeds most actively (Fig. 5d). The high concentration level of calcium and phosphorus near the granules facilitates the

diffusion of these elements to the center of the implant, which is necessary for the osteoid tissue to form. With insufficient concentration of calcium and phosphorus ions, the apatite phase appears mainly on the surface of the granules and adsorbs, thanks to its irregular surface, calcium phosphate precipitates—the precursors [7, 11, 12]. The growth of the bone matrix depends on the volume of the granules, the degree of carbonate substitution, and the presence of morphogenetic proteins that are adsorbed on the porous surface and stimulate the osteointegration of the material, i.e., its coalescence with the native bone [13].

It was established in the earlier *in vitro* studies [14] that the greatest activity of osteoblasts—the cells building up bone tissues—occurs on the surface of CHA containing 8.2 wt % CO_3^{2-} (study of the samples with 5.4–11.3 wt% CO_3^{2-} [14]), which roughly agrees with the results obtained in this work.

One can also note that the weak cellular infiltration into the granules might be due to the small size (less than 10 μm) of their near-surface pores, the optimum pore size for osteogenesis being 300–400 μm [15].

CONCLUSIONS

The results of our studies have shown that, as the concentration of carbonate groups in apatite is increased, its microstructure undergoes reconstruction from a dense, uniform dendritic pattern to a lamellar-acicular one and then to the formation of hexagonal crystals, accompanied by an increase in the solubility of granules. This makes for a more active *in vivo* formation of bone tissue. Histological investigations involving long-term observations have confirmed the bioactivity of CHA granules, the most favorable behavior being exhibited by the granules containing carbonate groups in a concentration of 6 wt %. Such granules can be used both as individual matrices and as part of composite materials based on cements and biopolymers.

ACKNOWLEDGMENTS

This work was supported by the Russian Foundation for Basic Research (grant no. 06-03-32192) and the President of the Russian Federation (grant no. MK 4047.2008.3, “Young Russian Scientists, Candidates of Sciences, and Their Advisers”).

REFERENCES

1. LeGeros, R.Z., Tung, M.S., Chemical Stability of Carbonate- and Fluoride-Containing Apatites, *Caries Res.*, 1983, vol. 17, pp. 419–429.
2. Dziedzic, D.M., Savva, I.H., Wilkinson, D.S., Davies, J.E., Osteoconduction on, and Bonding to, Calcium Phosphate Ceramic Implants, *Proc. Symp. Mater. Res. Soc.*, 1996, vol. 414, pp. 147–156.
3. Hasegawa, M., Sudo, A., Komlev, V.S., et al. High Release of Antibiotic from a Novel Hydroxyapatite with Bimodal Pore Size Distribution, *Biomed. Mater. Res., Part B: Appl. Biomater.*, 2004, vol. 70, pp. 332–339.
4. Komlev, V.S., Barinov, S.M., Porous Hydroxyapatite Ceramics of Bi-Modal Pore Size Distribution, *J. Mater. Sci.: Mater. Med.*, 2002, vol. 13, pp. 295–299.
5. Komlev, V.S., Peryn, F., Mastrogiacomo, M. et al, Kinetics of *in vivo* Bone Deposition by Bone Marrow Stromal Cells into Porous Calcium Phosphate Scaffolds; an x-ray Computed Microtomography Study, *Tissue Eng.*, 2006, vol. 12, pp. 3449–3458.
6. Ong, J.L., Hoppe, C.A., Cardenas, H.L. et al., Osteoblast Cell Activity on HA surfaces of Different Treatments, *J. Biomed. Mater. Res.*, 1998, vol. 39, pp. 176–183.
7. Barinov, S.M., Komlev, V.S., Biokeramika na osnove fosfatov kal'tsiya (Bioceramic Based on Calcium Phosphate), Moscow: Nauka, 2005.
8. Murugan, R., Sampath, T., Yang, F., Ramakrishna, S., Hydroxyl Carbonapatite Hybrid Bone Composites Using Carbohydrate Polymer, *J. Compos. Mater.*, 2005, vol. 39, pp. 1159–1166.
9. LeGeros, R.Z., Trautz, O.R., LeGeros, J.P. et al., Apatite Crystallites: Effects of Carbonate on Morphology, *Science*, 1967, vol. 155, pp. 1409–1411.
10. Porter, A., Patel, N., Brooks, R. et al., Effect of Carbonate Substitution on the Ultrastructural Characteristics of Hydroxyapatite Implants, *J. Mater. Sci. Mater. Med.*, 2005, vol. 16, pp. 899–907.
11. Krut, M.C., de Bruijn, J.D., Yuan, H. et al., Optimization of Bone Tissue Engineering in Goats: a Perforative Seeding Method Using Cryopreserved Cells and Localized Bone Formation in Calcium Phosphate Scaffolds, *Transplantation*, 2004, vol. 77, pp. 359–365.
12. Radin, S.R., Ducheyne, P., The Effect of Calcium-Phosphate Ceramic Composition and Structure on *in vitro* Behavior. II. Precipitation, *J. Biomed. Mater. Res.*, 1993, vol. 27, pp. 35–45.
13. Hing, K., Bone Repair in the Twenty-First Century: Biology, Chemistry of Engineering? *Phil. Trans. R. Soc. London A*, 2004, vol. 362, pp. 2821–2850.
14. Merry, J.C., Gibson, I.R., Best, S.M. et al., Synthesis and Characterization of Porous Hydroxyapatite, *J. Mater. Sci. Mater. Med.*, 1998, vol. 9, no. 12, pp. 779–783.
15. Tsuruga, E., Takita, H., Itoh, H. et al., Pore Size of Porous Hydroxyapatite as the Cell-Substratum Controls BMP-Induced Osteogenesis, *J. Biochem.*, 1997, vol. 121, pp. 317–324.